INSTITUTE OF NUCLEAR PHYSICS

Feasibility Study of $Be_{12}Ti$ as a Neutron Reflector in Nuclear Reactors

D.S. Sairanbayev[1], A.A. Shaimerdenov[1], S.V. Udartsev[2]

[1]Institute of Nuclear Physics, Kazakhstan

[2]Kazatomprom, Kazakhstan

JAEA

Joint IGORR 22nd/ IAEA Technical Meeting, 15-19 June, Mito, Japan

IAEA

AGENDA

- Introduction. Beryllium “poisoning”. Titanium beryllide
- WWR-K research reactor
- Materials and Methods
- Results
  - Reactivity margin and xenon poisoning
  - Neutron flux and spectral Distribution
  - Power distribution in reflectors
  - Isotope Production in Reflector Materials
  - Temperature Coefficients and Fuel Burnup
- Conclusion

INTRODUCTION. BERYLLIUM “POISONING”. TITANIUM BERYLLIDE

Metallic Beryllium (Be)

- d= 1.89 g/cc
- At%(Be)= 98.6

JENDL-5

$^{9}_{4}Be\ (n,\alpha)\ ^{6}_{2}He,$ 9.419 (mb)

$^{6}_{2}He \xrightarrow{\beta-} {}^{6}_{3}Li,$

940.4 (b) $^{6}_{3}Li\ (n,\alpha)\ ^{3}_{1}H,$ $T_{1/2}$=12.32 y

$^{3}_{1}H \xrightarrow{\beta-} {}^{3}_{2}He,$

5328 (b) $^{3}_{2}He\ (n,p)\ ^{3}_{1}H$

$^{9}_{4}Be\ (n,2n)\ 2^{4}_{2}He$

$^{9}_{4}Be\ (n,n')\ 2^{4}_{2}He$

(1 ÷ 6) x 10^{22} n/cm^2

E_n > 0.1 MeV

- Swelling (up to 50%)
- Embrittlement
- Cracking
- Deformation

Titanium Beryllide ($Be_{12}Ti$)

- d= 2.3 g/cc
- At%(Be)=92.3

$^{46}Ti(n,p)^{46}Sc$

$^{47}Ti(n,d+np)^{46}Sc$ $T_{1/2}$=83.79 d

$^{47}Ti(n,p)^{47}Sc$

$^{48}Ti(n,d+np)^{47}Sc$ $T_{1/2}$=3.35 d

$^{48}Ti(n,p)^{48}Sc$

$^{49}Ti(n,d+np)^{48}Sc$ $T_{1/2}$=43.71 h

- Swelling (up to 3%)
- ~~Embrittlement~~
- ~~Cracking~~
- ~~Deformation~~

KAZATOMPROM
ULBA
Ulba Metallurgical Plant
Joint-Stock Company

WWR-K Research Reactor

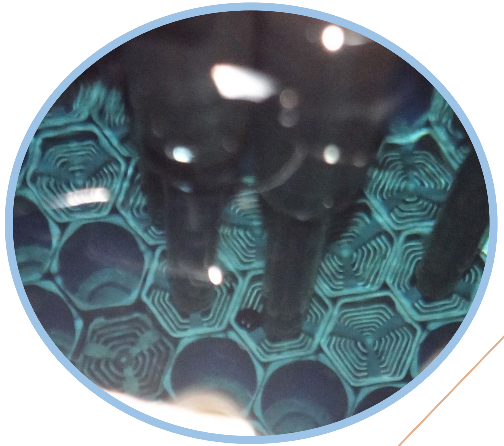

Thermal power: **6MW**
Fuel: **UO_2-Al**
Moderator, coolant: **light water**
Reflector: **metallic beryllium**
Enrichment ^{235}U: **19.7%**
Operation: **10 cycles/year**
1 operation cycle: **21 continuous days**

- Commissioned in 1967 (HEU fuel)
- Continuous operation till 1988
- 1988-1998 - safety upgrade, licensing
- Re-started in 1998
- 2015-2016 – Modernization and Conversion to LEU fuel
- April 1st 2016 – First Criticality with LEU fuel
- September 2016 – Operation of reactor with LEU fuel

Utilization

- NAA
- Fuel testing
- Gemstone radiation treatment
- Medical & industrial isotopes
- Neutron radiography & tomography
- Material science
- Neutron transmutation doping of silicon

MATERIALS AND CALCULATIONS

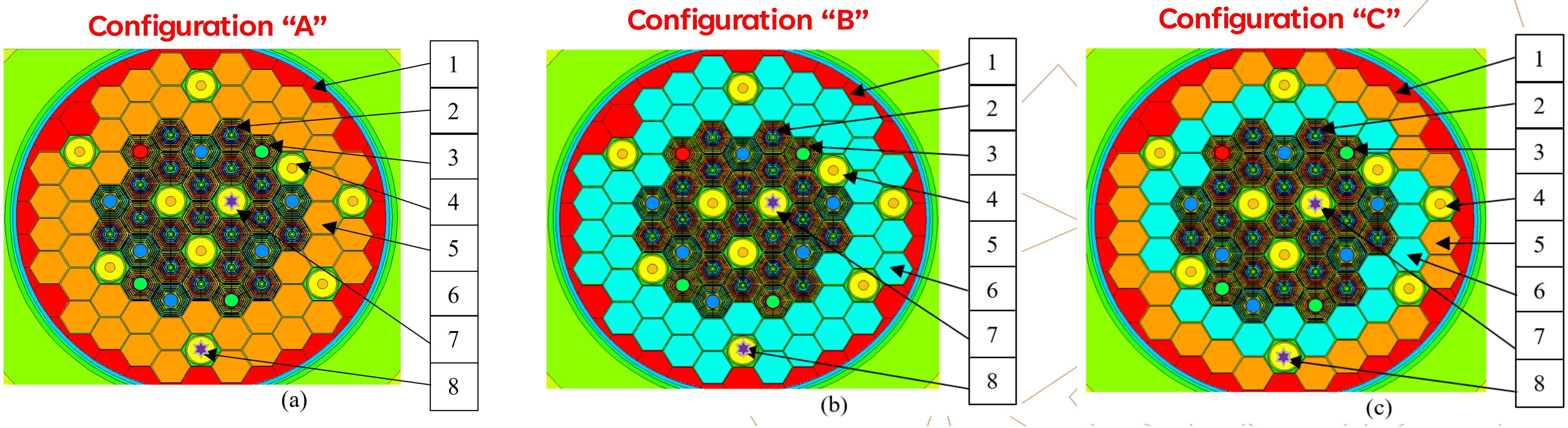

Figure 1 Horizontal sections of MCNP core models with different reflectors: (a) – two rings of metallic Be; (b) – two rings of $Be_{12}Ti$; (c) – the first ring of $Be_{12}Ti$, the second of metallic Be; (1) – water; (2) – type 1 fuel assemblies, (3) – type 2 fuel assemblies, (4) – irradiation channel, (5) – metallic Be, (6) – $Be_{12}Ti$, (7) – central irradiation position, (8) – peripheral irradiation position.

MCNP6

ENDF B-VII.1

- Reactivity margin ($\Delta k/k$)
- Neutron flux spectra (100 energy groups) at central and peripheral irradiation channels
- Power deposition in reflector blocks
- Production of isotopes: He-3, He-4, T, Li-6 in Be; Sc-46, Sc-47, Sc-48 in $Be_{12}Ti$
- Temperature coefficient of reactivity
- U-235 burnup in fuel assemblies

REACTIVITY MARGIN AND XENON POISONING

- Configuration A: Two rings of metallic Be (baseline)
- Configuration B: Two rings of $Be_{12}Ti$
- Configuration C: Hybrid: Inner ring of $Be_{12}Ti$ and outer ring of Be

Table 1. Calculated reactivity margin data [% Δk/k]

ρ (water)	ρ (“A”)	ρ (“B”)	ρ (“C”)
0.40±0.01	11.06±0.01 (~+10.6)	3.84±0.01 (~+3.4)	4.29±0.01 (~+3.9)

+ 14 fresh fuel
– 14 blocks

Be superior moderating and reflecting properties

the lower moderation efficiency

The calculated reduction in reactivity margin due to Xe-135 poisoning was:

- “A”: −2.75% Δk/k
- “B”: −2.97% Δk/k
- “C”: −2.94% Δk/k

the highest poisoning effect due to its harder neutron spectrum

NEUTRON FLUX AND SPECTRAL DISTRIBUTION

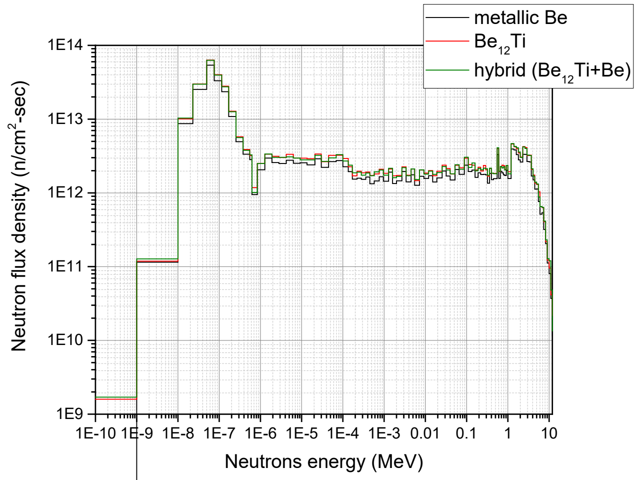

Figure 2. Neutron flux density for the 100-group energy spectrum at the central irradiation position

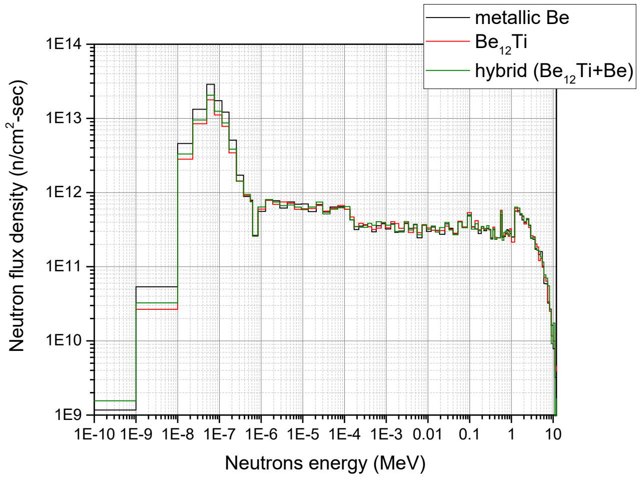

Figure 3. Neutron flux density for the 100-group energy spectrum at the peripheral irradiation position

Table 4. Thermal, epithermal and fast neutron flux densities at the central irradiation position [n/cm²-s]

central irradiation position			
Energy group	core configuration with reflectors		
	metallic Be	$Be_{12}Ti$	$Be_{12}Ti$+Be
Thermal neutrons (E_n<6.25 eV)	1.67E+14	1.98E+14 (+19%)	1.96E+14 (+17%)
Epithermal neutrons (E_n=(6.25 eV÷0.11 MeV))	7.96E+13	9.57E+13 (+20%)	9.40E+13 (+18%)
Fast neutrons (E_n>0.11 MeV)	6.94E+13	8.37E+13 (+21%)	8.36E+13 (+20%)

Table 5. Thermal, epithermal and fast neutron flux densities at the peripheral position [n/cm²-s]

peripheral irradiation position			
Energy group	core configuration with reflectors		
	metallic Be	$Be_{12}Ti$	$Be_{12}Ti$+Be
Thermal neutrons (E_n<6.25 eV)	8.50E+13	5.48E+13 (−35%)	6.18E+13 (−27%)
Epithermal neutrons (E_n=(6.25 eV÷0.11 MeV))	1.82E+13	1.84E+13 (+1%)	1.84E+13 (+1%)
Fast neutrons (E_n>0.11 MeV)	1.01E+13	1.03E+13 (+2%)	1.05E+13 (+4%)

POWER DISTRIBUTION IN REFLECTORS

Table 6. Power deposition values of the reflector blocks with different core configurations.

Block position No	Configuration		
	metallic Be	$Be_{12}Ti$	$Be_{12}Ti$+Be
1	3.4	4.6	4.7
2	6.0	7.2	7.2
3	3.9	4.4	4.4
4	6.6	7.2	7.2
5	4.9	5.8	5.8
6	4.2	5.0	5.1
7	3.5	4.9	5.0
8	4.1	5.0	5.1
9	6.4	7.8	7.8
10	3.9	5.6	5.7
11	4.2	4.8	4.8
...	…	…	…
22	4.1	4.4	4.4
23	1.9	3.8	2.8
24	2.1	3.7	2.7
...	…	…	…
42	1.5	2.3	1.7

- For the configuration using metallic Be, the total power deposition across all 46 reflector blocks was 137.7 kW. The highest localized deposition occurred near the fuel assemblies and irradiation positions, consistent with high neutron flux regions.
- In the case of the $Be_{12}Ti$ reflector, the total power deposition increased to 184.0 kW – approximately 34% higher than the Be configuration. This rise is attributed to $Be_{12}Ti$'s higher neutron absorption cross-section and heavier atomic mass, which contribute to greater local heating. Notably, the peripheral blocks of the Be12Ti reflector exhibited power levels exceeding 7.5 kW in some positions.
- The hybrid configuration (inner ring of $Be_{12}Ti$, outer ring of Be) demonstrated intermediate power deposition totaling 168.5 kW. This reflects the combined moderation characteristics of both materials and indicates that $Be_{12}Ti$'s influence on heating is substantial even when partially integrated.

ISOTOPE PRODUCTION IN REFLECTOR MATERIALS

Table 6. Production of isotopes Li-6, He-3, He-4 and T with different core configurations [at/barn-cm]

Configuration with metallic Be			
Isotopes	Cycles number		
	1	5	10
Li-6	1.53E-07	6.76E-07	1.16E-06
T	5.02E-09	1.09E-07	3.00E-07
He-3	1.04E-11	7.06E-09	1.19E-07
He-4	1.02E-06	5.19E-06	1.06E-05
Configuration with $Be_{12}Ti$			
Isotopes	Cycles number		
	1	5	10
Li-6	1.34E-07	6.36E-07	1.19E-06
T	1.87E-09	4.39E-08	1.45E-07
He-3	3.96E-12	1.29E-09	2.76E-08
He-4	8.75E-07	4.41E-06	8.90E-06
Configuration with ($Be_{12}Ti$+Be)			
Isotopes	Cycles number		
	1	5	10

Table 7. Production of Sc-46, Sc-47 and Sc-48 isotopes with different core configurations [GBq]

Configuration with $Be_{12}Ti$			
Isotopes	Cycles number		
	1	5	10
Sc-46	49.1	163.2	214.5
Sc-47	133.4	134.0	134.0
Sc-48	6.9	6.9	6.9
Configuration with ($Be_{12}Ti$+Be)			
Isotopes	Cycles number		
	1	5	10
Sc-46	48.9	162.4	213.3
Sc-47	132.8	133.4	133.4
Sc-48	6.9	6.9	6.9

TEMPERATURE COEFFICIENTS AND FUEL BURNUP

Table 9. Temperature reactivity feedback coefficients

Core configuration	αT (%Δk/k)/K)
with metallic Be	-0.007
with $Be_{12}Ti$	-0.010
with ($Be_{12}Ti$+Be)	-0.011

Table 9. The proportion of uranium-235 burnup in fuel assemblies in different core configurations [%]

Central FA			
Configuration	Cycles number		
	1	5	10
metallic Be	4.0	19.7	38.0
$Be_{12}Ti$	4.8	23.2	44.0
($Be_{12}Ti$+Be)	4.7	22.9	43.6
Peripheral FA			
Configuration	Cycles number		
	1	5	10
metallic Be	2.5	12.6	25.2
$Be_{12}Ti$	2.1	10.5	21.2

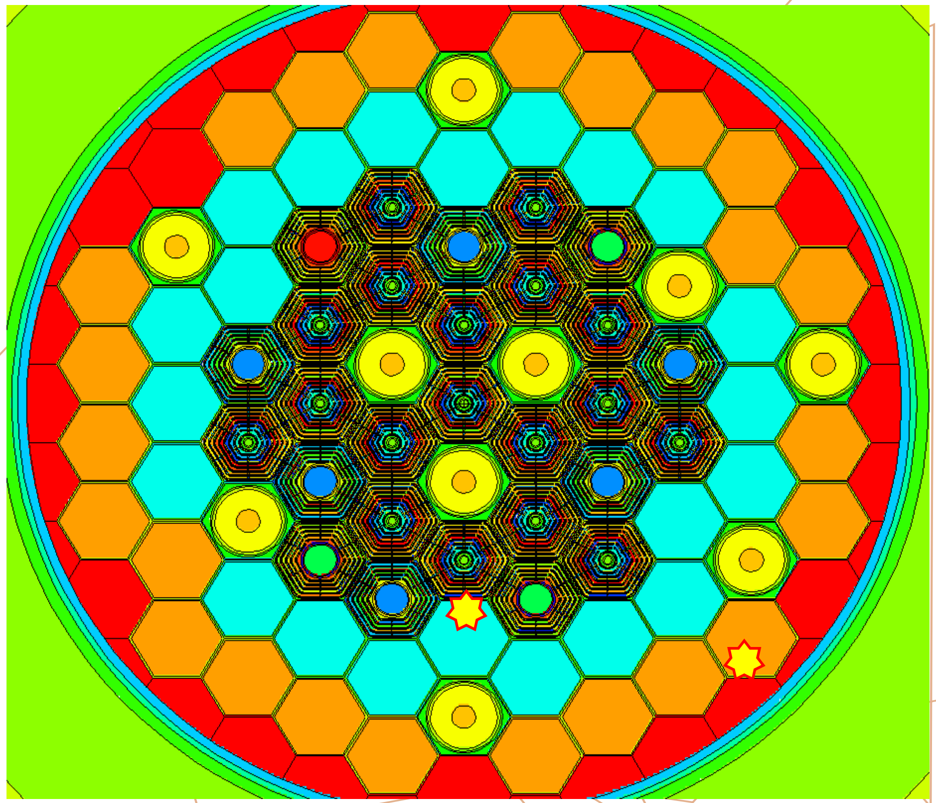

Core configuration	"A"	"B"	"C"
Overall average burnup [%]	2.94	2.94	2.94
Burnup [GWd/MTU]	4.01	4.01	4.01

CONCLUSIONS

This study provides a comparative neutronic analysis of three reflector configurations—metallic Be, titanium beryllide ($Be_{12}Ti$), and a hybrid of $Be_{12}Ti$ and Be—in the WWR-K research reactor. Results from MCNP simulations allow the following conclusions to be drawn:

Reactivity Margin: Metallic Be provides the **highest** initial reactivity margin. However, $Be_{12}Ti$ and hybrid configurations show reduced margins, and additional fresh fuel loading (e.g., 14 blocks for configuration B) would be required to match the Be configuration. Xenon poisoning further reduces reactivity in all configurations, most significantly in $Be_{12}Ti$.

Neutron Flux Distribution: Be yields the highest thermal flux in peripheral channels, ideal for isotope production. Be12Ti shifts the spectrum toward epithermal and fast ranges, enhancing fast flux but lowering thermal flux. The hybrid offers a balanced flux spectrum suitable for mixed applications.

Energy Deposition: Power deposition is highest in $Be_{12}Ti$ (184.0 kW), followed by the hybrid (168.5 kW) and Be (137.7 kW). Thermal management requirements increase with the inclusion of $Be_{12}Ti$.

Isotope Production: Metallic Be reflectors result in significantly higher He and T production. $Be_{12}Ti$ minimizes gas accumulation but introduces Sc-46, Sc-47, and Sc-48 through Ti activation. The hybrid effectively mitigates both issues.

Temperature Coefficients and Burnup: All configurations yield negative temperature coefficients, with $Be_{12}Ti$ and hybrid being more negative, enhancing inherent safety. Burnup analysis shows increased U-235 depletion in $Be_{12}Ti$ and hybrid cores, necessitating careful fuel cycle planning.

Overall, while Be provides optimal reactivity and thermal performance, $Be_{12}Ti$ offers structural and safety advantages at the cost of reactivity and power deposition. The hybrid configuration emerges as a viable compromise, balancing neutronic, thermal, and activation characteristics for multipurpose research reactor applications.

REFERENCES

[1] Van Renterghem, W., Leenaers, A., & Van denBerghe, S. (2008). TEM investigation of long-term annealed highly irradiated beryllium. Journal of Nuclear Materials, 374(1–2), 54–60. https://doi.org/10.1016/j.jnucmat.2007.07.007.
[2] Chakin, V. P., Kazakov, V. A., Melder, R. R., Goncharenko, Yu. D., & Kupriyanov, I. B. (2002). Effects of neutron irradiation at 70–200°C in beryllium. Journal of Nuclear Materials, 307–311, 647–652. https://doi.org/10.1016/s0022-3115(02)01218-7.
[3] Shaimerdenov, A., Sairanbayev, D., Kulsartov, T., Gizatulin, S., Akhanov, A., Zaurbekova, Z., Askerbekov, S., Dikov, A., Larionov, A., Udartsev, S., Kylyshkanov, M., & Podoinikov, M. (2023a). Irradiation experiments of titanium beryllide samples in the WWR-K reactor. Annals of Nuclear Energy, 194, 110120. https://doi.org/10.1016/j.anucene.2023.110120.
[4] Shaimerdenov, A., Akhanov, A., Gizatulin, Sh., Nessipbay, A., Shakirov, B., Askerbekov, S., Kulsartov, T., Kenzhina, I., Larionov, A., Akayev, S., & Udartsev, S. (2024). Effect of low-temperature neutron irradiation on the properties of Titanium Beryllide. Nuclear Materials and Energy, 38, 101582. https://doi.org/10.1016/j.nme.2024.101582.
[5] Frants, Y., Borsuk, A., Vechkutov, A., Zenkov, K., Zorin, B., Kylyshkanov, M., Podoinikov, M., Udartsev, S., Vladimirov, P., & Gaisin, R. (2022). Titanium beryllide as an alternative to beryllium in nuclear and thermonuclear engineering, capabilities of UMP JSC in the technology development and Beryllides Products Manufacture. Journal of Physics: Conference Series, 2155(1), 012015. https://doi.org/10.1088/1742-6596/2155/1/012015.
[6] Shaimerdenov, A.A., Nakipov, D.A., Arinkin, F.M., Gizatulin, S.K., Chakrov, P.V., Ye, A., 2018. Kenzhin the 50th anniversary of the WWR-K research reactor //. Physics of Atomic Nuclei 81 (10), 1408–1411. https://doi.org/10.1134/S1063778818100162
[7] Arinkin F.M., Shaimerdenov A.A., Gizatulin Sh.Kh., Dyussambayev D.S., Koltochnik S.N., Chakrov P.V., Chekushina L.V. WWR-K research reactor core conversion. – Atomic Energy, 2017, Vol.123 – p.15-20. DOI: 10.1007/s10512-017-0294-0.
[8] J.T. Goorley, et al., 2013. Initial MCNP6 Release Overview - MCNP6 version 1.0, LA-UR- 13-22934.
[9] M.B. Chadwick, M. Herman, P. Oblo˘zinský, M.E. Dunn, Y. Danon, A.C. Kahler, D.L. Smith, B. Pritychenko, G. Arbanas, R. Arcilla, R. Brewer, D.A. Brown, R. Capote, A.D. Carlson, Y.S. Cho, H. Derrien, K. Guber, G.M. Hale, S. Hoblit, S. Holloway, T.D. Johnson, T. Kawano, B.C. Kiedrowski, H. Kim, S. Kunieda, N.M. Larson, L. Leal, J.P. Lestone, R.C. Little, E.A. McCutchan, R.E. MacFarlane, M. MacInnes, C.M. Mattoon, R.D. McKnight, S.F. Mughabghab, G.P.A. Nobre, G. Palmiotti, A. Palumbo, M.T. Pigni, V.G. Pronyaev, R.O. Sayer, A.A. Sonzogni, N.C. Summers, P. Talou, I.J. Thompson, A. Trkov, R.L. Vogt, S.C. van der Marck, A. Wallner, M.C. White, D. Wiarda, P.G. Young, “ENDF/B-VII.1: Nuclear Data for Science and Technology: Cross Sections, Covariances, Fission Product Yields and Decay Data”, Nucl. Data Sheets 112(2011)2887.

FUNDING

This research was funded by the Committee of Science of the Ministry of Science and Higher Education of the Republic of Kazakhstan (Grant No. BR24993119).

THANK YOU FOR YOUR ATTENTION

Darkhan Sairanbayev, PhD

Laboratory of Atomic Energy Safety Problems

d.sairanbayev@inp.kz